

SCIENTIFIC REPORTS

OPEN

CRISPR/Cas9-based knockouts reveal that CpRLP1 is a negative regulator of the sex pheromone PR-IP in the *Closterium peracerosum-strigosum-littorale* complex

Naho Kanda¹, Machiko Ichikawa¹, Ayaka Ono², Atsushi Toyoda³, Asao Fujiyama³, Jun Abe², Yuki Tsuchikane², Tomoaki Nishiyama⁴ & Hiroyuki Sekimoto^{1,2}

Heterothallic strains of the *Closterium peracerosum-strigosum-littorale* (*C. psl.*) complex have two sexes, mating-type plus (mt^+) and mating-type minus (mt^-). Conjugation between these two sexes is regulated by two sex pheromones, protoplast-release-inducing protein (PR-IP) and PR-IP Inducer, which are produced by mt^+ and mt^- cells, respectively. PR-IP mediates the release of protoplasts from mt^- cells during mating. In this study, we examined the mechanism of action of *CpRLP1* (*receptor-like protein 1*), which was previously identified in a cDNA microarray analysis as one of the PR-IP-inducible genes. Using CRISPR/Cas9 technology, we generated *CpRLP1* knockout mutants in mt^- cells of the *C. psl.* complex. When the knockout mt^- cells were mixed with wild-type mt^+ cells, conjugation was severely reduced. Many cells released protoplasts without pairing, suggesting a loss of synchronization between the two mating partners. Furthermore, the knockout mutants were hypersensitive to PR-IP. We conclude that *CpRLP1* is a negative regulator of PR-IP that regulates the timing of protoplast release in conjugating *C. psl.* cells. As the first report of successful gene knockout in the class Charophyceae, this study provides a basis for research aimed at understanding the ancestral roles of genes that are indispensable for the development of land plants.

Sexual reproduction occurs in a wide variety of organisms, including plants, animals, and fungi. In sexual reproduction, haploid gametes of different types, which are genetically or developmentally determined, recognize each other and fuse to form a diploid zygote. In contrast to our increasing understanding of molecular mechanisms associated with sexual reproduction in higher plants^{1,2}, the evolution of these processes is still uncertain. Land plants are thought to have evolved from ancestors in charophycean algae^{3,4}. Charophycean algae are paraphyletic and contain six monophyletic lineages: Charales, Coleochaetales, Zygnematales, Klebsormidiales, Chlorokybales, and Mesostigmatales. Until now, genomic information has only been reported in *Klebsormidium nitens* NIES-2285 (Formerly *K. flaccidum*)⁵, however, some transcriptomic analyses are reported using some members of charophyceans^{6,7}. Recent phylogenetic analyses indicated that Zygnematales are the closest living relatives of land plants^{8,9}.

To study the molecular mechanism of sexual partner recognition in charophycean algae, we focused on the *Closterium peracerosum-strigosum-littorale* complex (*C. psl.* complex), a member of the order Zygnematales. The *C. psl.* complex is one of the most widely studied unicellular charophycean algae in terms of sexual reproduction^{10,11}. Furthermore, a technique for the stable transformation of the *C. psl.* complex has been developed^{12,13} and

¹Graduate School of Science, Japan Women's University, 2-8-1 Mejirodai, Bunkyo-ku, Tokyo, 112-8681, Japan.

²Faculty of Science, Japan Women's University, 2-8-1 Mejirodai, Bunkyo-ku, Tokyo, 112-8681, Japan. ³Center for Information Biology, National Institute of Genetics, 1111 Yata, Mishima, Shizuoka, 411-8540, Japan. ⁴Advanced Science Research Center, Kanazawa University, Takaramachi 13-1, Kanazawa, Ishikawa, 920-0934, Japan. Correspondence and requests for materials should be addressed to H.S. (email: sekimoto@fc.jwu.ac.jp)



Figure 1. Immunological detection of CpRLP1 protein in *C. psil.* complex cells. **(a)** CpRLP1 expression during sexual reproduction. Cells of the *mt*⁺ and *mt*⁻ strains were co-incubated in nitrogen-depleted medium and CpRLP1 levels were monitored by immunoblot analysis at various time points after co-incubation. **(b)** Cells of the *mt*⁻ strain were incubated in nitrogen-depleted medium containing PR-IP. Protein was isolated at regular time intervals and subjected to SDS-PAGE followed by immunoblotting with anti-CpRLP1 antibodies.

its genome is currently being sequenced. Heterothallic strains of the *C. psil.* complex have two morphologically indistinguishable sexes, mating-type plus (*mt*⁺) and mating-type minus (*mt*⁻). Sexual reproduction is readily induced when cells of the two sexes are cultured together in nitrogen-depleted medium under light. Sexual reproduction between *mt*⁺ and *mt*⁻ cells is regulated by two sex pheromones, namely protoplast-release-inducing protein (PR-IP) and PR-IP Inducer. PR-IP is produced by *mt*⁺ cells and induces protoplast release from *mt*⁻ cells. Conversely, PR-IP Inducer is produced by *mt*⁻ cells and induces the production of PR-IP in *mt*⁺ cells. As a result of the pheromonal communication, cells of opposite mating-types form a pair and release their protoplasts to form a zygote (Fig. S1). We recently proposed a possible sexual reproduction mechanism in the *C. psil.* complex^{11,14}. However, the receptors for these sex pheromones and the mechanism of the signal transduction have not been characterized yet.

A cDNA microarray analysis revealed 88 pheromone-inducible, conjugation-related and/or sex-specific genes¹⁵. Among them, we focused on two genes named *CpRLK1* and *CpRLP1* because *CpRLK1* encodes a receptor-like protein kinase (RLK), whereas *CpRLP1* encodes a leucine-rich repeat (LRR) receptor-like protein (RLP). The expression of *CpRLK1* in *mt*⁺ cells was stimulated by the PR-IP Inducer. While the function of *CpRLK1* was characterized using knockdown *mt*⁺ transformants of *CpRLK1* generated by the expression of antisense RNA¹³, the role of *CpRLP1* was not shown experimentally.

Because *CpRLP1* was a sole *mt*⁻ specific receptor-related gene found by the cDNA microarray analysis, we initially speculated that CpRLP1 might transduce the extracellular signal of PR-IP to the intracellular compartment. However, *CpRLP1* expression was elevated in response to application of PR-IP itself¹⁵, suggesting that a more complex mechanism could be at work. In this study, we analyzed transformants expressing antisense *CpRLP1* RNA and knockout lines generated by the newly established CRISPR/Cas9 system to determine the physiological function of *CpRLP1*. We report that *CpRLP1* knockout mutants showed a significant loss of conjugation and were hypersensitive to PR-IP. We conclude that CpRLP1 regulates the timing of protoplast release, which is required for cell fusion, possibly through inhibiting the action of PR-IP.

Results and Discussion

Characterization of CpRLP1. Because the *CpRLP1* cDNA in the EST database was a partial clone (DNA Database in Japan (DDBJ) accession no. AU295384), we cloned the full-length cDNA (2,108 bp) of this gene using 5' RACE-PCR (DDBJ accession no. LC309274). The predicted CpRLP1 protein was composed of 589 amino acid residues with a molecular mass of 60,578 Da (Fig. S2). A signal peptide directing the protein to the endoplasmic reticulum (1–32 aa) and a transmembrane domain (525–547 aa) were predicted (www.ebi.ac.uk/interpro/). The predicted extracellular domain contained 7 putative asparagine-linked glycosylation sites and 10 putative leucine-rich repeat (LRR) domains. The predicted cytoplasmic region (548–589 aa) was short and lacked a protein kinase domain.

To detect the presence of CpRLP1 in samples containing a combination of mating types, we prepared antibodies against a cocktail of two synthetic peptides (402-FGGPPRGEPEYFKDD-415, 435-DTDAADGGFSEGGAG-449) based on the extracellular domain of CpRLP1. CpRLP1 was immunologically detected as a band of approximately 75 kDa; this is a little larger than the predicted size (60,758 Da), probably due to glycosylation. The proteins were detected 4 h after the mating types were mixed (Fig. 1a). The intensity of the signal increased up to 12 h after mixing and then gradually declined. CpRLP1 accumulated in *mt*⁻ cells that had been incubated with PR-IP (Fig. 1b). CpRLP1 protein was detected as 100-, 150-, and 250-kDa bands when SDS-PAGE was performed without reducing reagent (Fig. S3), suggesting that CpRLP1 forms heterodimers with unknown molecules or homodimers through disulfide bonds.

Evaluation of phenotypes of knockdown transformants. To investigate the role of *CpRLP1* in cell conjugation, we constructed a knockdown vector, pSA0104_anti-*CpRLP1* (Fig. S4). Antisense *CpRLP1* cDNA was cloned under the control of the native *CpHSP70* promoter (*pCpHSP70*) and introduced in *mt*⁻ cells via particle bombardment. The transformed cells were selected for hygromycin resistance and six *mt*⁻ transformants were isolated. In a previous work, we demonstrated that the *pCpHSP70* was constitutively active and useful for driving foreign genes¹⁶. So, we hypothesized that the *pCpHSP70* promoter would drive expression of antisense *CpRLP1*

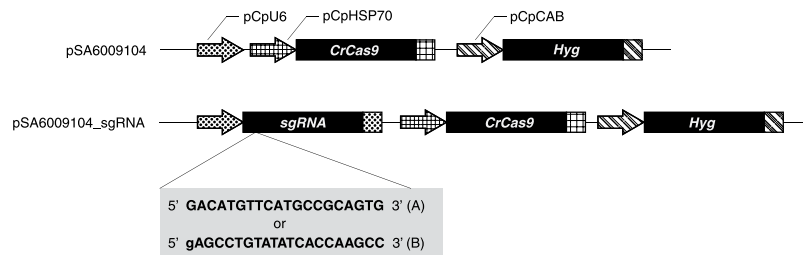


Figure 2. *Cas9* vector constructs with and without the *pCpU6*-*sgRNA* cassette. *Chlamydomonas* codon-optimized *Cas9*, *sgRNA*, and *Hyg* are under the control of the *pCpHSP70*, *pCpU6-1*, and *pCpCAB1* promoters, respectively. The plasmid backbone is pBluescript II SK⁺. An extra G at the 5' end of the *sgRNA* sequence for *sgRNA_B* was added because the *U6* promoter requires a G for the start of transcription.

RNA and thereby reduce CpRLP1 protein levels. When mt⁻ transformants were incubated with wild-type mt⁺ cells, the resulting sexual phenotypes varied, with some having higher rates of conjugation than others (Fig. S5). Three transformants (A1H, A4H, and A11H) had reduced levels of mating and reduced expression of *CpRLP1* compared to the control transformant, which was transformed using empty pSA0104 vector. However, we did not get a line in which the *CpRLP1* was suppressed nearly completely so that the protein was not detectable in western blotting. Thus the observed phenotype could be weaker than what will be observed with a null allele mutant.

Isolation of CRISPR/Cas9-induced *CpRLP1* mutants. Because a null allele mutation might cause a clearer phenotype than antisense RNA technology, we used the CRISPR/*Cas9* system to knock out *CpRLP1* expression in mt⁻ cells. We introduced the pSA6009104_*sgRNA_A* and *_B* vectors (Fig. 2) into the mt⁻ cells of the *C. ps.* complex. Transformants were selected on media containing 50 µg/ml hygromycin. Eight clonal lines were established for the two constructs. pSA6009104, which lacks the *sgRNA* sequence, was introduced as a negative control.

To confirm that the *CpRLP1* sequence was disrupted in the clonal transformants, genomic DNA spanning the target sequences was PCR amplified and sequenced. All clonal transformants showed dual sequence peaks within the target site, suggesting the presence of two copies of *CpRLP1* in the *C. ps.* complex NIES-68 genome. We analyzed the mutation patterns in target DNA cloned from each strain, and detected two mutation patterns in each strain (Fig. 3). Among the eight strains, three (A-2, B-2, and B-4) showed frameshift mutations in two respective gene copies and were considered to be complete *CpRLP1*-knockout mutants.

Phenotypic characterization of *CpRLP1* mutants. The transformants were incubated with wild-type mt⁺ cells for 8 h and CpRLP1 accumulation was assayed using immunoblot assays. We detected two bands of around 75 kDa in close proximity to each other in the negative control (Fig. 4a). Both bands were absent in strains with frameshift mutations in both *CpRLP1* genes (A-2, B-2, and B-4). The bands were less prominent in strains in which only one of the *CpRLP1* genes might be functional; only the upper band was detected in B-3, B-5, and B-6, whereas both bands were detected at extremely low levels in A-1 and B-1 (Fig. 4a). Because of the presence of both bands in A-1 and B-1, in which one of the *CpRLP1* genes was disrupted, we concluded that the upper and lower bands did not correspond to the respective gene copies. Instead, the differences in protein accumulation patterns among these strains probably reflect differences in protein structure introduced by the mis-sense mutations or small deletions. Whereas strain A-1 had no change in target region B and strain B-1 had a single substitution in target region B, strains B-3, B-5, and B-6 all lacked TKPGLLK in target region B. Thus, the TKPGLLK sequence is possibly important for proper protein conformation and for the protein's ability to function as a substrate that can be modified, resulting in faster electrophoretic mobility (e.g. dephosphorylation).

We examined the mating behaviors of transformed mt⁻ and wild-type mt⁺ cells after 48 h of co-incubation. We counted the number of mating cells (i.e., pair-forming cells, protoplast-releasing cells from the pair, and zygote-forming cells) and the number of protoplast-releasing cells without pairing (lone protoplast-releasing cells). Strains in which *CpRLP1* expression was completely absent (A-2, B-2, and B-4) and strains in which only the upper band was detected by immunoblotting (B-3, B-5, and B-6) mated less frequently than the control (vector-transformed control mt⁻ cells combined with wild-type mt⁺ cells; Fig. 4b). Significant differences were calculated using the generalized linear model (GSM) in R 3.2.3. (**p value < 0.001,¹⁷). In the case of the A-1 and B-1 strains, which exhibited faint lower bands in the immunoblot, mating was slightly inhibited. These data suggest that the protein represented by the lower MW band is of greater significance for the progression of mating than is the other protein. Reduced mating is consistent with the phenotype of knockdown lines that had less CpRLP1 accumulation (Fig. S5), though the degree of inhibition was smaller.

In addition to the reduced mating reaction, all transformants showed a relatively high ratio of lone protoplast-releasing cells to total cells compared to the control (GSM, *p-value < 0.01, **p value < 0.001). It is known that mt⁻ cells but not mt⁺ cells occasionally release the lone protoplasts without pairing during sexual reproduction in the *C. ps.* complex¹⁸ and that the lone protoplast release is induced by the sex pheromone, PR-IP, which is released by mt⁺ cells^{10,14}. The observation that the *CpRLP1* mutants had relatively higher rates of protoplast release without pairing than did the wild type suggests that the *CpRLP1* mutants impair the normal response to the PR-IP. The mt⁻ cells can be induced to release protoplasts in the absence of mt⁺ cells by the addition of purified PR-IP¹⁸. When the control transformant was exposed to various amounts of purified PR-IP, the

AA	N A D M F M P Q W G G M G D I C G P L G	Mutation Type	Protein
WT	5'- AACGCCGACATGTTTCATGCCGCA—GTGGGGCGGCATGGGCGACATCTGCGCCCGCTGGGG -3'	-	NADMFMFPQWGGMGDICGPLG
A-1	5'- AACGCCGACATGTTTCATGCCGCAAGTGGGGCGGCATGGGCGACATCTGCGCCCGCTGGGG -3'	1 insertion	NADMFMFPVGRHGRHLRPAAG
	5'- AACGCCGACATGT—GGGGCGGCATGGGCGACATCTGCGCCCGCTGGGG -3'	12 deletion	NADM—WGGMGDICGPLG
A-2	5'- AACGCCGACATGTTTCATGCCGCA—TGGGCGACATCTGCGCCCGCTGGGG -3'	11 deletion	NADMFMPHGRHLRPAAGVGGAR
	5'- AACGCCGACATGTTTCATGCCGCA—CGGGG -3'	32 deletion / 1 change	NADMFMHPGVGARGDVRHDR
AA	L S S L Y I T K P G L L K T I K Q L T	Mutation Type	Protein
WT	5'- CTGAGCAGCTGTATATACCAA—GCCCGGGCTGCTCAAACGATCAAGCAGCTCACGG -3'	-	LSSLYITK-PGLLTIKQLT
B-1	5'- CTGAGCAGCTGTATATACCAA—TGCCCGGGCTGCTCAAACGATCAAGCAGCTCACGG -3'	1 insertion	LSSLYITNARAAQNDQAAHA
	5'- CTGAGCAGCTGTATATACCCGA—GCCCGGGCTGCTCAAACGATCAAGCAGCTCACGG -3'	1 change	LSSLYITE-PGLLTIKQLT
B-2	5'- CTGAGCAGCTGTATATCAC—CCCGGGCTGCTCAAACGATCAAGCAGCTCACGG -3'	4 deletion	LSSLYITPGCKSRSSSSRSL
	5'- CTGAGCAGCTGTATATACCAA—ACCGCGTCTCAAACGATCAAGCAGCTCACGG -3'	1 deletion / 2 changes	LSSLYITKARAAQNDQAAHA
B-3	5'- CTGAGCAGCTGTATATACCAA—AACGATCAAGCAGCTCACGG -3'	15 deletion	LSSLYIT—TIKQLT
	5'- CTGAGCAGCTGTATATACCAAAGCAGCCGGGCTGCTCAAACGATCAAGCAGCTCACGG -3'	3 insertion	LSSLYITKQPGLLTIKQLT
B-4	5'- CTGAGCAGCTGTATATACCAA—AGCCCGGGCTGCTCAAACGATCAAGCAGCTCACGG -3'	1 insertion	LSSLYITKARAAQNDQAAHA
	5'- CT—AGCCCGGGCTGCTCAAACGATCAAGCAGCTCACGG -3'	20 deletion / 1 change	LSSPGCKSRSSSSRSLTRST
B-5	5'- CTGAGCAGCTGTATATCAGC—CCCGGGCTGCTCAAACGATCAAGCAGCTCACGG -3'	4 deletion / 1 change	LSSLYISPGCKSRSSSSRSL
	5'- CTGAGCAGCTGTATATACCAA—AACGATCAAGCAGCTCACGG -3'	15 deletion	LSSLYITK—TIKQLT
B-6	5'- CTGAGCAGCTGTATATACCAA—AGCCCGGGCTGCTCAAACGATCAAGCAGCTCACGG -3'	1 insertion	LSSLYITKARAAQNDQAAHA
	5'- CTGAGCAGCTGTATATACCAA—AAGGATCAAGCAGCTCACGG -3'	15 deletion / 1 change	LSSLYITK—RIKQLT

Figure 3. Overview of CRISPR/Cas9-induced mutations in *CpRLP1*. The wild-type (WT) sequence is shown with the protospacer adjacent motif (PAM) sequence in orange and the sgRNA target sequences (target region A and B) in blue. The corresponding amino acid (AA) sequence is depicted above the nucleotide sequence. Deletions are denoted using red dashes. Insertions and nucleotide substitutions are indicated in red letters. The amino acid sequences of the target region are listed on the right, and the altered sequences are indicated using red letters and dashes.

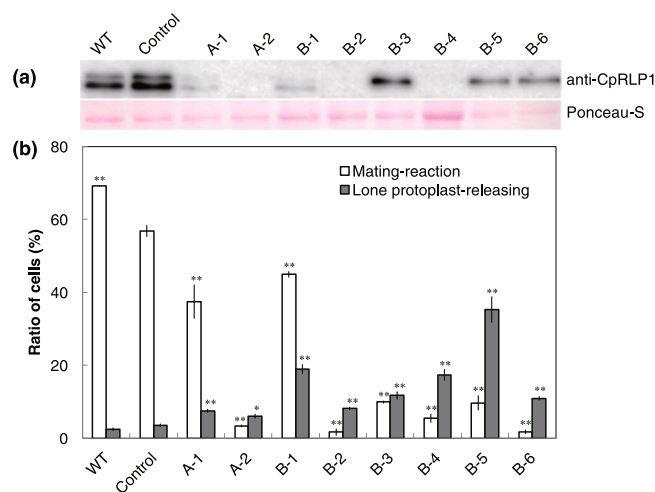


Figure 4. Characterization of CRISPR/Cas9-mediated *CpRLP1* knockout mutants. (a) Immunoblotting with anti-CpRLP1 antibodies. mt^- cells (wild-type, control strain, or CRISPR/Cas9-mediated *CpRLP1* mutants) were incubated with wild-type mt^+ cells for 8 h. Protein lysates were prepared and subjected to SDS-PAGE. Ponceau-S-stained protein bands are shown as a loading control. (b) Status of cells 48 h after mixing. Cells exhibiting a mating reaction (pairing, protoplast-releasing from the pair, and zygote-forming cells) and lone protoplast-releasing cells are indicated by white bars and gray bars, respectively. The data represent averages of three independent experiments. Significant differences compared to the control (i.e., vector-transformed control mt^- cells combined with wild-type mt^+ cells) were calculated using the generalized linear model (GLM) in R 3.2.3. and are indicated with an asterisk (*p-value < 0.01, **p value < 0.001). Vertical bars indicate SE.

ratio of protoplast-releasing cells to total cells increased with increasing concentrations of PR-IP up to 0.3 $\mu\text{g}/2\text{ ml}$. However, the ratio decreased with a further increase in PR-IP concentration. These results are in agreement with our previous study¹⁸. By contrast, the release of protoplasts by the *CpRLP1* knockout mutants peaked at 0.1 μg PR-IP/2 ml and decreased at higher concentrations of PR-IP (Fig. 5, Fig. S6).

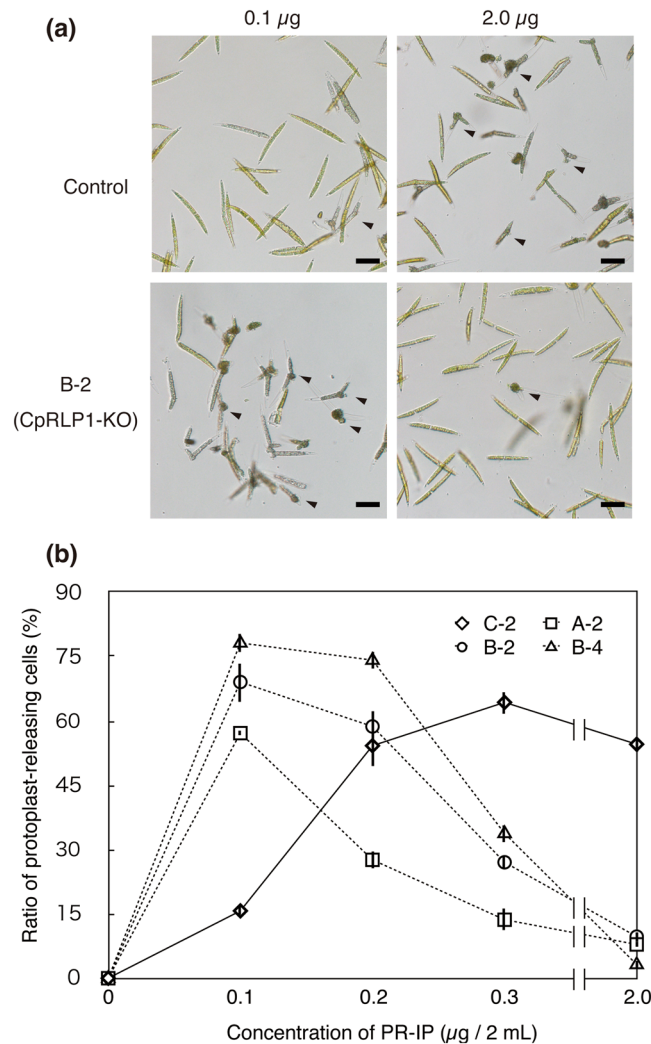


Figure 5. Effect of PR-IP on the induction of protoplast release. **(a)** Photographs of control and CRISPR/Cas9-mediated *CpRLP1* knockout mt^- cells (CpRLP1-KO) incubated with various concentrations of PR-IP. The amount of PR-IP per 2 ml of MI medium is shown above, and the names of strains are indicated to the left. Arrowheads indicate protoplast-releasing cells. Scale bar = 50 µm. **(b)** Proportion of cells releasing protoplasts in the presence of various concentrations of PR-IP. The dashed and solid lines represent data for the *CpRLP1* knockout strains (A-2, B-2, and B-4) and control strain (C-2), respectively. The data represent averages of three independent experiments. Vertical bars indicate SE.

The observation that mutants mated with wild-type mt^+ cells could be explained as follows: the knockout mt^- cells are hypersensitive to PR-IP secreted from the mt^+ cells. While some of the knockout cells released their protoplasts without pairing, most cells did not because the local concentration of PR-IP was high enough to prevent the mutant cells from releasing protoplasts.

Conclusion and perspective. In this study, we successfully established a CRISPR/Cas9-based gene knock-out system for the *C. psil.* complex. Using this system, we revealed the phenotypes of *CpRLP1* knockout mutants and evaluated the role of *CpRLP1* in successful mating of the *C. psil.* complex. Knockout of *CpRLP1* markedly elevated the sensitivity of mt^- cells to PR-IP, suggesting that *CpRLP1* acts as a negative regulator of PR-IP. With the knockdown phenotype alone appeared difficult to reach this conclusion because some activity was remaining and the phenotypes were thus weak, although the reduced mating phenotype was consistent with both experiments.

Based on results described here and previously^{19,20}, we postulate that the following series of events occurs during sexual reproduction in the *C. psil.* complex. Under conditions that favor mating, mt^- cells differentiate into sexually competent cells¹⁹ and an unknown receptor for the 19-kDa subunit of PR-IP appears on the cell surface²⁰. Once PR-IP is detected by the receptor, the mt^- cells start to express genes such as *CpRLP1* that facilitate the progression of sexual reproduction¹⁵. As a result, *CpRLP1* appears on the cell surface and might form a heterodimer with the receptor (or a homodimer with itself). Following formation of the dimer, the hypersensitivity to PR-IP is reduced, which in turn, mediates protoplast release after sexual pair formation.

In general, it is considered that RLPs form receptor-complexes with RLKs and are involved in the adaptation to environmental changes and the developmental programs through the specific recognition of ligands^{21–25}, however, only a few RLPs have been functionally characterized^{21,26}; e.g. CLAVATA^{27,28} and TOO MANY MOUSE (TMM)^{29,30} etc.

Recently, we identified *CpRLK2* from an EST database and found that the extracellular domain of the deduced protein shares 40% amino acid sequence similarity with that of *CpRLP1*. The position of cysteine residues was largely conserved between *CpRLP1* and *CpRLK2*. Because this gene is expressed only in sexually differentiated mt⁻ cells, it may be a receptor for PR-IP and may form a heterodimer with *CpRLP1*, like as a case of ERECTA family receptor kinases and TMM²⁹. We are now trying to establish *CpRLK2* knockout mutants to confirm that *CpRLK2* is a receptor for PR-IP. In addition, the heterodimerization of *CpRLP1* and *CpRLK2* as well as the binding of PR-IP to *CpRLK2* and/or *CpRLP1*, should be demonstrated to clarify the mechanism of PR-IP-reception and negative regulation by *CpRLP1*. In conclusion, this work contributes to our understanding of signaling mechanisms during the sexual reproduction of the *C. psil.* complex. Not restricted in the *C. psil.* complex, we believe that our reverse genetics approach using the CRISPR/Cas9 system can be used to characterize unknown genes in the order Zygnematales.

Methods

Strains and vegetative culture conditions. Strains of heterothallic *Closterium peracerosum-strugosum-littorale* complex (*C. psil.* complex) used in this study included NIES-67 (mt⁺) and NIES-68 (mt⁻). These were obtained from the National Institute for Environmental Studies (Ibaraki, Japan). Vegetative cells were cultured in nitrogen-supplemented medium (C medium; <http://www.nies.go.jp/biology/mcc/home.htm>), as previously described¹⁸.

Mating culture conditions. Sexual reproduction was induced in vegetative cells of the *C. psil.* complex that had been cultured for two weeks (late-logarithmic phase). The cells were harvested, washed three times with nitrogen-depleted medium (MI medium;³¹), and incubated separately in 72 ml of fresh MI medium in 300 ml Erlenmeyer flasks (1.0×10^5 cells ml⁻¹) under continuous light (110 μ mol photons m⁻² s⁻¹) for 24 h (pre-culture). Pre-cultured cells of both mating types (1.0×10^5 each) were mixed in 2 ml fresh MI medium. After 48 h incubation, cells were fixed using 0.6% glutaraldehyde and the number of cells undergoing sexual reproduction were counted using an Olympus IX83 inverted microscope (www.olympus-ims.com) with a UPlanFLN4xPH, UPlanFLN10 \times 2PH, or LUCPlanFLN20xPH objective lens. Images were captured using a DP80 digital camera system and cellSens Dimension software (ver. 1.9, Olympus). The experiments were repeated at least three times. Significant differences were calculated using the generalized linear model (GLM) in R 3.2.3¹⁷. For immunoblot analysis, pre-cultured cells of both mating types (3.0×10^6 each) were mixed in 72 ml fresh MI medium in 300 ml Erlenmeyer flasks, and harvested as described¹³ at 4, 8, 12, 16, 20, 24, 48, and 72 h after the mixing.

Cloning of *CpRLP1* cDNA and sequence analysis. Complete sequences of EST clones (4-01G01, CL27_E10, and E-41) spanning part of *CpRLP1*¹⁵ were determined using the Multi-capillary Automated DNA Sequencer CEQ 2000XL (Beckman Coulter, www.meretics.com) according to the manufacturer's instructions. cDNA synthesis from total RNA was performed using a 5'-RACE System for Rapid Amplification of cDNA Ends Kit (Invitrogen, www.lifetechnologies.com) according to the manufacturer's instructions. The 5' regions of genes were amplified using a gene-specific primer (4-01G01-3') and 5'-RACE anchor primer (Invitrogen). The PCR conditions were 95 °C for 2 min; 35 cycles at 95 °C for 0.5 min, 57 °C for 45 s, and 72 °C for 5 min; and 72 °C for 5 min using Ex taq (Takara Bio, www.takara-bio.com). Nested PCR using the diluted PCR product was performed using a gene-specific primer (4-01G01-5'-race) and universal amplification primer (Invitrogen). The PCR products were separated on a 1.5% agarose gel, collected using the SUPREC 01 column (Takara), ligated into the pGEM T-easy vector (Promega, www.promega.com), and transformed into DH5 α *E. coli* cells. Plasmid DNA was purified using the QIAprep Spin Miniprep Kit (Qiagen, www.qiagen.com/). Using sequence information from the insert DNA, full-length cDNA was amplified from primary cDNA prepared using a GeneRacer Kit with a 4-01G01-S1 primer and a GeneRacer 3' primer. The PCR conditions were 95 °C for 2 min; 5 cycles at 95 °C for 0.5 min, 72 °C for 4 min; 5 cycles at 95 °C for 0.5 min, 70 °C for 4 min; 22 cycles at 95 °C for 0.5 min, 68 °C for 4 min; and 68 °C for 10 min. Full-length cDNA was cloned into the pGEM T-easy vector and the sequence was confirmed. The sequence was deposited in the DNA Data Bank of Japan (DDBJ) under the accession number LC309274. All primer sequences used in this study are listed in Table S1. Sequence analysis was performed using the Genetyx software package (Software Development, www.genetyx.co.jp). The deduced protein sequence was analyzed using InterPro program (<http://www.ebi.ac.uk/Tools/pfa/iprscan/>).

Construction of *CpRLP1*-knockdown vectors. To construct the pSA0102_anti-*CpRLP1* vector, *CpRLP1* cDNA was PCR amplified from the cDNA clone using *CpRLP1*-5'-*Bam*HI and *CpRLP1*-3'-*Spe*I primers (Table S1) and inserted between the *Bam*HI and *Spe*I sites of pSA0102¹³ in the antisense direction using a Ligation Kit (Takara Bio, www.takara-bio.com) according to the manufacturer's instructions. To construct the pSA0104_anti-*CpRLP1* vector, pSA0102_anti-*CpRLP1* was digested with *Xba*I and *Xho*I and the *CpRLP1* fragment was inserted between the *Kpn*I and *Eco*RI sites of the pSA0104 vector¹³ using a GENEART Seamless Cloning and Assembly Kit (Life Technologies, www.lifetechnologies.com) according to the manufacturer's instructions.

All PCRs for plasmid construction were carried out using KOD-plus NEO DNA polymerase (TOYOBO, lifesience.toyobo.co.jp). Amplified PCR products were purified using a High Pure PCR Cleanup Micro Kit (Roche, roche-biochem.jp) according to the manufacturer's instructions. Primer sequences used in this study are listed in Supplemental Table S1. The sequences of the resulting plasmids and direction of the inserts were verified using the CEQ8000 Genetic Analysis System (Beckman Coulter, www.beckmancoulter.co.jp) and the DTCS-Quick Start Kit (Beckman).

Construction of *Cas9* vector targeting *CpRLP1*. Based on the preliminary genome database of the *C. psil.* complex, which is composed of raw sequence read data (DRA005947, DDBJ), we identified three putative *U6* snRNA genes. One of these genes was amplified from genomic DNA of mt⁻ cells using gene-specific primers (CpU61-S1-geneart and CpU61-A1-geneart, Table S1) and was cloned into the *Bam*HI and *Eco*RI sites of the pBluescript II SK⁺ vector using a Gibson Assembly Cloning Kit (New England Biolabs, www.neb.com) according to the manufacturer's instructions. The sequence was deposited in DDBJ under the accession number LC310798. The sequence was highly conserved among various organisms (Fig. S7).

To create pSA6009104, a codon-optimized version of *Cas9* from *Chlamydomonas reinhardtii* (*CrCas9*) was used³², because the codon usage of the *C. psil.* complex is similar to that in *C. reinhardtii*¹⁶. *CrCas9* was PCR amplified using *CrCas9*-5-geneart and *CrCas9*-3-geneart primers and cloned into the *Xho*I site of the pSA0104 vector¹³, downstream of the *CpHSP70* gene promoter, using a GENEART Seamless Cloning and Assembly Kit. Then, the region of the *CpU6-1* promoter upstream of the endogenous *Kpn*I site was PCR amplified using CpU6-F-geneart and CpU6-R-geneart primers and cloned into the *Kpn*I site of the vector containing *CrCas9*. This vector was named pSA6009104 for CRISPR/*Cas9*-mediated editing of the *C. psil.* complex (Fig. 2).

Two sgRNA sequences for *CpRLP1* (sgRNA_A: 350-GACATGTTTCATGCCGAGTG-369, and sgRNA_B: 542-AGCCTGTATATACCAAGCC-561; Fig. S1) were selected in the N-terminal region of the *CpRLP1* coding sequence using the "Guide RNA Target Design Tool" (<https://www.blueheronbio.com/external/tools/gRNASrc.jsp>). Two sgRNA expression cassettes containing a 120-bp fragment of the *CpU6-1* promoter downstream of the endogenous *Kpn*I site, one of the two target sequences for sgRNA, and the sgRNA scaffold were synthesized commercially (FASMAC, www.fasmac.co.jp) and inserted into the pSA6009104 vector. For sgRNA_B, an extra G at the 5' end of the sgRNA sequence was added because the *U6* promoter requires a G for the start of transcription³³.

Transformation of the *C. psil.* complex. The constructs were linearized using *Not*I restriction endonuclease and the DNA was introduced into mt⁻ cells using particle bombardment as described³⁴. Eight independent clonal lines were established by picking a single cell from hygromycin-resistant colonies.

Detection of target site mutations in *CpRLP1*. Genomic DNA was extracted as described³⁴. *CpRLP1* genomic DNA was PCR amplified using RLP1-S1 and RLP1-A1 primers, and cloned between the *Eco*RI and *Bam*HI sites of the pBluescript II SK⁺ vector using a Gibson Assembly Cloning Kit. The sequence was determined using RLP1-S2 and RLP1-S4 primers for target A and B, respectively.

Preparation of anti-CpRLP1 antibody and immunoblot analysis using anti-CpRLP1 antibody. Two synthetic peptides (A: Cys-⁴⁰²FGGPPRGEPYFKDD⁴¹⁵, B: Cys-⁴³⁵DTDAADGGFSEGGAG⁴⁴⁹) that include part of the CpRLP1 extracellular domain were used as antigens. Two rabbits were immunized with both peptides conjugated to keyhole limpet hemocyanin. Antibodies specific to the peptides were purified using affinity columns (NHS-activated Sepharose 4 Fast Flow, GE Healthcare, www.gelifedciences.com) coupled with both peptide-A and -B. The purified antibody was divided into aliquots and stored at -80 °C until needed.

Cells undergoing sexual reproduction were harvested and disrupted as described¹³. Protein content of the cell lysates was measured using the Bradford method³⁵ with bovine serum albumin as the standard. The samples were subjected to SDS-PAGE using a 10% polyacrylamide gel. After electrophoresis, the proteins were transferred to a nitrocellulose membrane (Optitran BA-S 85, Whatman, www.gelifedciences.com) and probed with affinity-purified anti-CpRLP1-specific polyclonal antibody. Binding of the primary antibody was detected using a horseradish peroxidase-conjugated anti-rabbit IgG antibody (Methyl Laboratories, USA). CpRLP1 protein was detected by chemiluminescence using Versadoc (Bio-rad, USA) or the Odyssey Fc Imaging System (LI-COR, USA).

Purification and functional assay of PR-IP. PR-IP was purified as described previously¹⁸. The mt⁻ cells (1.0 × 10⁴ cells) that had been cultured for 24 h were incubated in 2 ml MI medium containing various concentrations of purified PR-IP. After 48 h of incubation, cells were fixed using 0.6% glutaraldehyde and the number of cells involved in the process of papillae formation and protoplast release were counted. Cell images were obtained using an Olympus microscope system (model IX-83).

Accession Numbers. Sequence data of *CpRLP1* cDNA and of *CpU6-1* genomic DNA can be found in the DNA Database in Japan (DDBJ) under accession numbers LC309274 and LC310798, respectively. Genomic sequence data for the NIES-68 strain can be found in the DDBJ under accession number DRA005947.

References

- Li, H. & Yang, W. C. RLKs orchestrate the signaling in plant male-female interaction. *Sci China Life Sci* **59**, 867–877, <https://doi.org/10.1007/s11427-016-0118-x> (2016).
- Higashiyama, T. & Yang, W. C. Gametophytic pollen tube guidance: attractant peptides, gametic controls, and receptors. *Plant Physiol* **173**, 112–121, <https://doi.org/10.1104/pp.16.01571> (2017).
- Graham, L. E., Graham, J. E. & Wilcox, L. W. *Algae 2nd ed.*, (Benjamin Cummings, 2009).
- Karol, K. G., McCourt, R. M., Cimino, M. T. & Delwiche, C. F. The closest living relatives of land plants. *Science* **294**, 2351–2353, <https://doi.org/10.1126/science.1065156> (2001).
- Hori, K. *et al.* *Klebsormidium flaccidum* genome reveals primary factors for plant terrestrial adaptation. *Nat. Commun.* **5**, 3978, <https://doi.org/10.1038/ncomms4978> (2014).
- Delaux, P. M. *et al.* Algal ancestor of land plants was preadapted for symbiosis. *Proc Natl Acad Sci USA* **112**, 13390–13395, <https://doi.org/10.1073/pnas.1515426112> (2015).
- Ju, C. *et al.* Conservation of ethylene as a plant hormone over 450 million years of evolution. *Nature Plants* **1**, 14004, <https://doi.org/10.1038/nplants.2014.4> (2015).
- Timme, R. E., Bachvaroff, T. R. & Delwiche, C. F. Broad phylogenomic sampling and the sister lineage of land plants. *PLoS One* **7**, e29696, <https://doi.org/10.1371/journal.pone.0029696> (2012).

9. Wickett, N. J. *et al.* Phylotranscriptomic analysis of the origin and early diversification of land plants. *Proc Natl Acad Sci USA* **111**, E4859–E4868 (2014).
10. Sekimoto, H., Abe, J. & Tsuchikane, Y. New insights into the regulation of sexual reproduction in *Closterium*. *Int. Rev. Cell Mol. Biol.* **297**, 309–338, <https://doi.org/10.1016/B978-0-12-394308-8.00014-5> (2012).
11. Sekimoto, H., Tsuchikane, Y. & Abe, J. In *Sexual Reproduction in Animals and Plants* (eds H. Sawada, N. Inoue, & M. Iwano) Ch. 28, 345–357 (Springer, 2014).
12. Abe, J. *et al.* Stable nuclear transformation of the *Closterium peracerosum-strigosum-littorale* complex. *Plant Cell Physiol.* **52**, 1676–1685, <https://doi.org/10.1093/pcp/pcr103> (2011).
13. Hirano, N. *et al.* A Receptor-like kinase, related with cell wall sensor of higher plants, is required for sexual reproduction in the unicellular charophycean alga, *Closterium peracerosum-strigosum-littorale* complex. *Plant Cell Physiol.* **56**, 1456–1462 (2015).
14. Sekimoto, H. Sexual reproduction and sex determination in green algae. *J. Plant Res.* **130**, 423–431, <https://doi.org/10.1007/s10265-017-0908-6> (2017).
15. Sekimoto, H. *et al.* Gene expression profiling using cDNA microarray analysis of the sexual reproduction stage of the unicellular charophycean alga *Closterium peracerosum-strigosum-littorale* complex. *Plant Physiol.* **141**, 271–279 (2006).
16. Abe, J., Hiwatashi, Y., Ito, M., Hasebe, M. & Sekimoto, H. Expression of exogenous genes under the control of endogenous *HSP70* and *CAB* promoters in the *Closterium peracerosum-strigosum-littorale* complex. *Plant Cell Physiol* **49**, 625–632 (2008).
17. R Core Team. R: A language and environment for statistical computing. *R Foundation for Statistical Computing, Vienna, Austria*. URL <http://www.R-project.org/>. (2016).
18. Sekimoto, H., Satoh, S. & Fujii, T. Biochemical and physiological properties of a protein inducing protoplast release during conjugation in the *Closterium peracerosum-strigosum-littorale* complex. *Planta* **182**, 348–354 (1990).
19. Sekimoto, H. & Fujii, T. Analysis of gametic protoplast release in *Closterium peracerosum-strigosum-littorale* complex (Chlorophyta). *J. Phycol.* **28**, 615–619 (1992).
20. Sekimoto, H., Satoh, S. & Fujii, T. Analysis of binding of biotinylated protoplast-release-inducing protein that induces release of gametic protoplasts in the *Closterium peracerosum-strigosum-littorale* complex. *Planta* **189**, 468–474 (1993).
21. Wang, G. *et al.* A genome-wide functional investigation into the roles of receptor-like proteins in *Arabidopsis*. *Plant Physiol* **147**, 503–517 (2008).
22. Wang, G. & Fiers, M. Receptor-like proteins: searching for functions. *Plant Signal Behav* **5**, 540–542, <https://doi.org/10.4161/psb.11030> (2010).
23. Monaghan, J. & Zipfel, C. Plant pattern recognition receptor complexes at the plasma membrane. *Curr. Opin. Plant Biol.* **15**, 349–357, <https://doi.org/10.1016/j.pbi.2012.05.006> (2012).
24. Shinohara, H. & Matsubayashi, Y. Reevaluation of the CLV3-receptor interaction in the shoot apical meristem: dissection of the CLV3 signaling pathway from a direct ligand-binding point of view. *Plant J* **82**, 328–336, <https://doi.org/10.1111/tjp.12817> (2015).
25. Jorda, L. *et al.* ERECTA and BAK1 receptor like kinases interact to regulate immune responses in *Arabidopsis*. *Front Plant Sci* **7**, 897, <https://doi.org/10.3389/fpls.2016.00897> (2016).
26. Lv, Y. *et al.* New insights into receptor-like protein functions in *Arabidopsis*. *Plant Signal Behav* **11**, e1197469, <https://doi.org/10.1080/15592324.2016.1197469> (2016).
27. Muller, R., Bleckmann, A. & Simon, R. The receptor kinase CORYNE of *Arabidopsis* transmits the stem cell-limiting signal CLAVATA3 independently of CLAVATA1. *Plant Cell* **20**, 934–946, <https://doi.org/10.1105/tpc.107.057547> (2008).
28. Zhu, Y. *et al.* Analysis of interactions among the CLAVATA3 receptors reveals a direct interaction between CLAVATA2 and CORYNE in *Arabidopsis*. *Plant J* **61**, 223–233, <https://doi.org/10.1111/j.1365-313X.2009.04049.x> (2010).
29. Lee, J. S. *et al.* Direct interaction of ligand-receptor pairs specifying stomatal patterning. *Genes Dev* **26**, 126–136, <https://doi.org/10.1101/gad.179895.111> (2012).
30. Lee, J. S. *et al.* Competitive binding of antagonistic peptides fine-tunes stomatal patterning. *Nature* **522**, 439–443, <https://doi.org/10.1038/nature14561> (2015).
31. Ichimura, T. In *Proceedings of the 7th International Seaweed Symposium* (ed. K. Nishizawa) 208–214 (University of Tokyo Press, 1971).
32. Jiang, W., Brueggeman, A. J., Horken, K. M., Plucinak, T. M. & Weeks, D. P. Successful transient expression of Cas9 and single guide RNA genes in *Chlamydomonas reinhardtii*. *Eukaryot Cell* **13**, 1465–1469 (2014).
33. Sander, J. D. & Joung, J. K. CRISPR-Cas systems for editing, regulating and targeting genomes. *Nat Biotechnol* **32**, 347–355 (2014).
34. Abe, J. *et al.* Preparation of knockdown transformants of unicellular charophycean alga, *Closterium peracerosum-strigosum-littorale* complex. *Bio-protocol* **6**, e1813 (2016).
35. Bradford, M. M. A rapid and sensitive method for the quantitation of microgram quantities of protein utilizing the principle of protein-dye binding. *Anal. Biochem.* **72**, 248–254 (1976).

Acknowledgements

We thank Drs Wenzhi Jiang and Donald P. Weeks for providing us with the *Chlamydomonas* codon-optimized Cas9 vector. We also thank Satoko Akatsuka, Mie Haduki, Makiko Hanasato, Tomomi Nakagawa, and Yuka Marukawa for their help in conducting preliminary experiments. This work was supported by Grants-in-Aid for Scientific Research (Nos 24370038, 26650147, 15H05237, 16H02518, 16H06378, 16H06279, and 16H04836 to H.S. and 26440223 to Y.T.) from the Japan Society for the Promotion of Science. This work was also supported in part by a KAKENHI (Grant-in-Aid for Scientific Research) for Innovative Areas “Genome Science” (No. 221S0002 to A.T. and A.F.) from the Ministry of Education, Culture, Sports, Science and Technology of Japan.

Author Contributions

H.S. conceived the project and supervised the experiments; H.S. and N.K. designed the research; N.K., M.I., A.O., and H.S. performed the experiments; J.A., Y.T., A.T. and A.F. generated the genome data; T.N. and H.S. analyzed the data; H.S., N.K., M.I., Y.T., J.A., and T.N. interpreted the results; and N.K. and H.S. wrote the paper with contributions from all authors.

Additional Information

Supplementary information accompanies this paper at <https://doi.org/10.1038/s41598-017-18251-8>.

Competing Interests: The authors declare that they have no competing interests.

Publisher's note: Springer Nature remains neutral with regard to jurisdictional claims in published maps and institutional affiliations.



Open Access This article is licensed under a Creative Commons Attribution 4.0 International License, which permits use, sharing, adaptation, distribution and reproduction in any medium or format, as long as you give appropriate credit to the original author(s) and the source, provide a link to the Creative Commons license, and indicate if changes were made. The images or other third party material in this article are included in the article's Creative Commons license, unless indicated otherwise in a credit line to the material. If material is not included in the article's Creative Commons license and your intended use is not permitted by statutory regulation or exceeds the permitted use, you will need to obtain permission directly from the copyright holder. To view a copy of this license, visit <http://creativecommons.org/licenses/by/4.0/>.

© The Author(s) 2017